FINE-SCALE ADAPTATIONS TO ENVIRONMENTAL VARIATION AND GROWTH STRATEGIES DRIVE PHYLLOSPHERE *METHYLOBACTERIUM* DIVERSITY.

Jean-Baptiste Leducq[1,2,3], Émilie Seyer-Lamontagne[1], Domitille Condrain-Morel[2], Geneviève Bourret[2], David Sneddon[3], James A. Foster[3], Christopher J. Marx[3], John M. Sullivan[3], B. Jesse Shapiro[1,4] & Steven W. Kembel[2]

1 - Université de Montréal
2 - Université du Québec à Montréal
3 – University of Idaho
4 – McGill University

Key words: *Methylobacterium* diversity, Phyllosphere community dynamics, *rpoB* barcoding, temperature adaptation, growth strategies in *Bacteria*

Abstract

Methylobacterium is one of the most prevalent bacterial genera of the phyllosphere, present on the leaves of nearly every plant. Despite its ubiquity and its importance for host plant function, little is known about whether diversity over space and time within the genus reflects neutral processes like migration and drift, or environmental filtering of life history strategies and adaptations to temperature and host tree species. Here, we investigated how phylogenetic diversity within the genus *Methylobacterium* is structured by biogeography, seasonality, and growth strategies. Using deep, culture-independent barcoded marker gene sequencing coupled with culture-based approaches, we quantified seasonal shifts in *Methylobacterium* diversity over a year from early summer to fall in two temperate forests in Québec, Canada. As an alternative to the 16S rRNA gene, we used *rpoB,* a highly polymorphic marker gene, which has not experienced detectable horizontal gene transfer nor copy number variation in *Methylobacterium* genomes. We cultured very different subsets of *Methylobacterium* diversity from the same leaf, depending upon the temperature of isolation and growth (20 °C or 30 °C). For instance, one the most abundant *Methylobacterium* lineages was almost exclusively isolated at 20 °C, suggesting long-term adaptation to temperature. Both culture and barcoding approaches revealed that a

considerable and previously underestimated diversity of *Methylobacterium* colonize the surface of leaves in temperate forests. This diversity was strongly structured according to both large (>100km; between forests) and small geographical scales (<1.2km within forests), and among host tree species, and was dynamic over seasonal time scales. To determine if these seasonal effects were driven by temperature, we measured growth of 79 isolates at different temperature treatments. Different lineages showed subtle and significant differences in growth performance when subject to temperature increase or decrease, but most have higher yield and slower growth rate at 20° than 30° C, with strong lineage- and season-dependant variation in their overall growth strategies. We proposed that the homogenization of *Methylobacterium* community structure observed over a growing season resulted from the progressive replacement of isolates with high yield strategy typical of cooperative, structured communities, by isolates with rapid growth. Together our results show how *Methylobacterium* is phylogenetically structured into lineages with distinct growth strategies, which helps explain their differential abundance across regions, host tree species, and time. This works paves the way for further investigation of adaptive strategies and traits within a ubiquitous phyllosphere genus.

Acknowledgments: FRQNT (funding), NSERC (funding), Canada Research Chairs (funding), NSF (DEB-1831838), Geneviève Lajoie, Dominique Tardif, Ariane Lafrenière, Hélène Dion-Phénix, Yves Terrat, Kenta Araya (help for sampling), Sylvain Dallaire (help for phenotyping screen), Sergey Stolyar (discussions), Gault Natural Reserve (McGill University), Station Biologique des Laurentides (UdeM), Centre d'Étude de la Forêt (CEF), QCBS.

Author contributions : J.B.L., E.S.L., D.C.M., G.B., B.J.S. and S.W.K. planned fieldwork and the experiments. J.B.L. E.S.L., D.C.M. and G.B. performed experiments. J.B.L. and E.S.L. performed bioinformatic analyses with contributions from D.S. and J.M.S. J.A.F., C.J.M. and J.M.S. provided discussion in the early stages of this study. J.B.L. B.J.S. and S.W.K. drafted the manuscript with contributions from C.J.M.

Data accessibility: raw reads for *16s* and *rpoB* barcoding on phyllosphere communities (BioProject PRJNA729807; BioSamples SAMN19164946-SAMN19165146) can be retrieved from NCBI under SRA Accession Numbers SRR14532212-SRR14532451. Partial nucleotide

63 sequences from marker genes obtained by SANGER sequencing on *Methylobacterium* isolates
64 (BioProject PRJNA730554 ; Biosamples SAMN19190155-SAMN19190401) can be retrieved
65 from NCBI under GenBank Accession Numbers MZ268514-MZ268593 (*16s*), MZ330152-
66 MZ330358 (*rpoB*) and MZ330130-MZ330151 (*sucA*).
67
68
69

Introduction

Phyllosphere, the aerial parts of plants including leaves, is a microbial habitat estimated as vaste as twice the surface of the earth [1]. Although exposed to harsh conditions, like UVs, temperature variations and poor nutrient availability, the phyllosphere arbors a diverse community of microorganisms, of which bacteria are the most abundant [1]. A key challenge in microbial ecology and evolution is understanding the evolutionary and ecological processes that maintain diversity in habitats such as the phyllosphere. Bacteria living in the phyllosphere carry out key functions including nitrogen fixation, growth stimulation and protection against pathogens [1–3]. At broad spatial and temporal scales, bacterial diversity in the phyllosphere varies as a function of biogeography and host plant species, potentially due to restricted migration and local adaptation to the biotic and abiotic environment [4–6], leading to patterns of cophylogenetic evolutionary association between phyllosphere bacteria and their host plants [7]. Whether those eco-evolutionary processes are important at short time scales, as microbes and their host plants migrate and adapt to changing climates, is still an open question [8]. Another challenge is to link seasonal variation with plant-associated microbial community dynamics, as shifts in microbial community composition are tighly linked with host plant carbon cycling [9] and ecosystem functions including nitrogen fixation [10]. More generally, we understand very little about how the ecological strategies of phyllosphere bacteria vary among lineages and in response to variation in environmental conditions throughout the growing season [9,11].

Phylogenetic signal in traits or suites of correlated traits that are used as indicators of the ecological life history strategy of microbes suggest niche adaptation [12], and these phenotypic traits influence the assembly of ecological communities through their mediation of organismal interactions with the abiotic and biotic environment [13]. Recent work evaluating the phylogenetic depth of microbial trait evolution has shown that many microbial phenotype traits exhibit phylogenetic signal, with closely related lineages possessing similar phenotypic traits, although the phylogenetic depth at which this signal is evident differs among traits [14]. Most comparative studies of microbial trait evolution have focused on broad scale patterns across major phyla and classes [14], although some studies have found evidence for complex patterns of phenotypic and genomic evolution within microbial genera interacting to determine patterns of community

101 assembly and niche evolution [15,16]. Furthermore, to date the majority of studies of the diversity of
102 plant-associated microbes have been based on the use of universal marker genes such as the
103 bacterial 16S rRNA gene, providing a global picture of long-term bacterial adaptation to different
104 biomes and host plants at broad phylogenetic scales [17], but lacking sufficient resolution to assess
105 the evolutionary processes at finer spatial and temporal scales that lead to the origin of and
106 adaptations within microbial genera and species [18,19].
107
108 The Rhizobiales genus *Methylobacterium* (*Alphaproteobacteria*, *Rhizobiales*,
109 *Methylobacteriaceae*) is one of the most prevalent bacterial genera of the phyllosphere, present
110 on nearly every plant [20,21]. Characterized by pink colonies due to carotenoid production,
111 *Methylobacterium* are facultative methylotrophs, able to use one-carbon compounds, such as
112 methanol excreted by plants, as sole carbon sources [21–23]. Experimental studies have shown the
113 important roles of *Methylobacterium* in plant physiology, including growth stimulation through
114 hormone secretion [24–26], heavy metal sequestration [26], anti-phytopathogenic compound secretion,
115 and nitrogen fixation in plant nodules [27], sparking increasing interest in the use of
116 *Methylobacterium* in plant biotechnology applications [26,28,29]. Although up to 64
117 *Methylobacterium* species have been described [30–38], genomic and phenotypic information was
118 until recently limited to a small number of model species: *M. extorquens, M. populi*, *M. nodulans*,
119 *M. aquaticum* and *M radiotolerans*, mostly isolated from anthropogenic environments, and only
120 rarely from plants [39–43]. Newly available genomic and metagenomic data now allow a better
121 understanding of *Methylobacterium* diversity across biomes [30], but we still understand relatively
122 little about the drivers of the evolution and adaptation of *Methylobacterium* in natural habitats.
123
124 In this study, we assessed the diversity of *Methylobacterium* in temperate forests and asked
125 whether *Methylobacterium* associated with tree leaves act as an unstructured population with
126 large effective size, or if this diversity was maintained by regional factors (*e.g.* a combination of
127 isolation by distance and regional environmental variation) or by niche adaptation (*e.g.* host tree
128 or temperature adaptation) [12]. First, we assessed *Methylobacterium* diversity by combining
129 culturing and barcoding approaches along with phylogenetic analysis and quantified how this
130 diversity varied across space, time, and environment in the phyllosphere. Second, we quantified
131 the extent of phylogenetic niche differentiation within the bacterial genus *Methylobacterium*,

132 with a focus on quantifying the evidence for adaptation to local environmental variation at
133 different spatial, temporal and phylogenetic scales. We hypothesized that distinct phylogenetic
134 lineages would be associated with distinct environmental niches. Third, we quantified
135 *Methylobacterium* growth performance under fine-scale environmental variations, with a focus
136 on temperature, to determine whether *Methylobacterium* diversity fine-scale dynamics over space
137 and time might result from environmental filtering of isolates with contrasting growth strategies
138 under local environmental conditions. We found that *Methylobacterium* phyllosphere diversity
139 consisted of deeply branching phylogenetic lineages associated with distinct growth phenotypes,
140 isolation temperatures, and large-scale spatial effects (forest of origin), while finer-scale spatial
141 effects, host tree species, and time of sampling were more weakly and shallowly phylogenetically
142 structured. Over the course of a year, from spring to fall, we observed a homogenization of
143 *Methylobacterium* community structure coinciding with the progressive replacement of isolates
144 with high yield strategy by isolates with rapid growth. Together our results show that this
145 ubiquitous phyllosphere genus is structured into lineages with distinct growth strategies, which
146 helps explain their differential abundance across space and time.
147
148 **Results**
149
150 *Phylogenetics of plant-associated Methylobacterium diversity.*
151
152 We evaluated the known *Methylobacterium* diversity associated with plants, especially the
153 phyllosphere, by compiling information about the origin of 153 *Methylobacterium* isolates for
154 which genomes were available. We found that plants (65% of genomes) and especially the
155 phyllosphere compartment (41% of genomes) were the most prevalent source of
156 *Methylobacterium*. From these genomes, we built a maximum-likelihood phylogenetic tree based
157 on the complete nucleotide sequence of *rpoB*, a highly polymorphic marker that experienced no
158 copy number variation in many bacteria taxa [44,45], and that we confirmed to be single copy in
159 *Methylobacterium* and related genera *Microvirga* and *Enterovirga* (**Figure 1, Table S1**). In this
160 phylogeny, we roughly identified main *Methylobacterium* groups (A, B, and C) previously
161 defined based on the 16S gene [30] and found that phyllosphere-associated diversity was not
162 randomly distributed in the *Methylobacterium* phylogenetic tree. Strains isolated from the

163 phyllosphere represented the largest part of diversity within group A (56% of strains) but not in
164 groups B and C (17 and 12% of strains, respectively). Most of diversity within group A consisted
165 of undescribed taxa falling outside previously well-described linages (**Figure 1, Table S1**). For
166 the purpose of this study, we refined *Methylobacterium* group A that we subdivided into 9
167 monophyletic clades (A1-A9), using a ~92% pairwise similarity (PS) cut-off on the *rpoB*
168 complete sequence (**Figure S1**).
169
170 *16S Community analyses reveal Methylobacterium ubiquity and diversity in the phyllosphere.*
171
172 We focused on *Methylobacterium* phyllosphere diversity variation observable at the scale of
173 seasonal variation on individual trees within a geographic region, the temperate forests of
174 northeastern North America. In two forests: Mont Saint Hilaire (MSH) and Station biologique
175 des Laurentides (SBL), we marked 40 trees representative of diversity observed in 4-6 plots
176 distributed along a 1.2 km transect (4-10 trees per plot). In MSH, the transect followed an
177 elevation and floristic gradient, while in SBL, it followed a relatively constant environment
178 (**Figure 2**). For this time series, each tree was sampled 3-4 times from June to October 2018. We
179 evaluated the microbial phyllosphere diversity in our time series based on sequencing and
180 identification of bacterial 16S gene amplicon sequence variants (ASVs; [46]) in a representative
181 subset of 46 phyllosphere samples from 13 trees (**Tables S2-S4, Figures S2,S3**). As observed in
182 previous studies [4], the distribution of the phyllosphere bacterial community was mostly explained
183 by differences among forests (31.6% of variation explained; $p<0.001$; PERMANOVA; Hellinger
184 transformation; 10,000 permutations), host tree species (15.6% of variation; $p<0.001$) and time of
185 sampling (12.0%; $p<0.05$; **Table S5, Figure S4**), indicating that between-forest variation and
186 adaptation to hosts were the main drivers of this diversity, which also varied greatly at the time
187 scale of a year. Although representing only 1.3% (0.0-3.2% per sample) of total 16S sequence
188 diversity, *Methylobacterium* was present in almost all analyzed samples (45 out of 46). We
189 assigned the 15 *Methylobacterium* ASVs identified by 16S sequencing to clades from
190 *Methylobacterium* group A: A9 (*M. phyllosphaerae/M. mesophilicum/M. phyllostachyos/ M.*
191 *pseudosasicola/M. organophilum;* 0.87% of total diversity, nine ASVs), A6 (*M. sp.*, 0.29%; one
192 ASV) and A1 (*M. gossipicola*; 0.13%, 3 ASVs; **Table S4**). With two rare ASVs (<0.01% of
193 relative abundance) assigned to *M. komagatae*, belonging to group A [30] but unrelated to any

194 aforementioned clade, we defined a new clade (A10). No ASV was assigned to group B or group
195 C, hence confirming observations from available genomes that *Methylobacterium* group A is
196 tightly associated with the phyllosphere.
197
198 *Development of a single-copy molecular marker to monitor fine-scale dynamics of*
199 *Methylobacterium populations.*
200
201 Although the 16S barcoding approach suggests that *Methylobacterium* is ubiquitous in the
202 phyllosphere of temperate forests, regardless of location, time and host tree species, identification
203 based on 16S sequencing presents some limits in assessing microbial population dynamics at
204 local scales, and in assessing fine-scale evolutionary adaptations [18]. First, the low polymorphism
205 of the 16S rRNA gene does not permit distinguishing among species within clades typical of the
206 phyllosphere, thus confounding species with potentially divergent evolutionary routes reflecting
207 the distinct ecological niches they occupy within the phyllosphere. Second, 16S copy number
208 variation within *Methylobacterium* (4-12) and even within groups of closely related strains (4-6
209 copies in group A; 5 in group B; 6-12 copies in group C), may induce biases in estimating
210 relative abundances of taxa, and thus in assessing the dynamics of populations over space, time
211 and among host tree species.
212
213 To assess *Methylobacterium* diversity at a finer evolutionary level, we thus developed a
214 molecular marker targeting all members of the *Methylobacteriaceae* family, using the core gene
215 *rpoB* (**Figure 1** [44,45]). Based upon *rpoB* sequences available for *Methylobacterium*, as well as
216 sequencing of *rpoB* partial sequences from 20 *Methylobacterium* strains isolated from a pilot
217 survey in MSH in 2017 (See supplementary information; **Figure 2, Tables S2,S6)**, we
218 determined that this gene is polymorphic enough to explore diversity within the aforementioned
219 *Methylobacterium* clades (**Table S7, Figure S5**). For the rest of this study, we used the *rpoB*
220 marker to monitor temporal trends in *Methylobacterium* diversity in the phyllosphere from our
221 2018 time series in both forests **(Figure 2, Table S3)**.
222
223 *Culture-based assessment of Methylobacterium diversity in the tree phyllosphere.*
224

225 We evaluated the culturable part of *Methylobacterium* diversity from a subsample of 36 trees (18
226 per forest) representative of floral diversity in the 2018 time series in MSH and SBL. To date,
227 *Methylobacterium* was mostly isolated assuming its optimal growth was in the range 25-30 °C [47],
228 an approach that could lead to a bias toward mesophylic isolates in estimating microbial
229 diversity, especially in the case of microbes inhabiting temperate forests where temperatures
230 typically range from 10 to 20 °C during the growing season [48]. We thus performed replicate
231 isolation of *Methylobacterium* at both 20 and 30 °C on minimum mineral salt (MMS) media with
232 0.1% methanol as sole carbon source. We successfully amplified the *rpoB* marker for 167 pink
233 isolates (**Tables S8-S10**) that we assigned to *Methylobacterium* based upon their phylogenetic
234 placement (**Figure S6)**. As observed for 16S ASVs, most isolates were assigned to clades from
235 group A typical of the phyllosphere: A9 (59.9% of isolates), A6 (24.6%), A1 (5.4%), A10 (3.6%)
236 and A2 (1.8%). Few isolates were assigned to group B (4.8% of isolates), mostly related to *M.*
237 *extorquens*, and none to group C. But the higher polymorphism in the *rpoB* marker allowed us to
238 uncover a considerable diversity within clades, as we identified 71 unique *rpoB* sequences, in
239 contrast to the smaller number obtained with 16S barcoding (15 ASVs).
240
241 Such high diversity in *rpoB* suggests that standing genetic variation is segregating within
242 *Methylobacterium* populations inhabiting the phyllosphere. We hypothesized that the
243 maintenance of this divestity could be explained by regional factors (*e.g.* a combination of
244 isolation by distance and regional environmental variation) and/or by niche adaptation (*e.g.* host
245 tree or temperature adaptation)[12]. To do so, we quantified associations between each ecological
246 factor and *Methylobacterium* diversity (at varying depths in the *rpoB* phylogeny; **Figure 3a**). For
247 each phylogenetic depth, we tested the association of each clade (with >50% bootstrap support;
248 see Methods; **Figure S7**) with four factors and their interactions (PERMANOVA with 10,000
249 permutations): (1) forest of sampling (2) temperature of isolation, (3) sampling time, and (4) host
250 tree species. For every phylogenetic depth tested, clades had distinct associations with forest of
251 origin (7.5±2.2% of variance explained; $p<0.001$) and temperature of isolation (7.2±1.6% of
252 variance explained; $p<0.001$; **Figure 3a**). Interestingly, temperature of isolation was the most
253 important factor distinguishing deep phylogenetic divergences (pairwise nucleotide
254 similarity<0.988), while forest of origin was slightly more important in structuring more recently
255 diverged clades. This suggests that mechanisms underlying isolation success at different

256 temperatures played a significant role in the early divergence among *Methylobacterium* clades
257 associated with tree leaves, while spatial variation among different forests evolved more recently.
258 Time of sampling had a slight but significant effect on diversity (2.4±0.2% of variance explained;
259 $p<0.05$) and it was observed at roughly the same phylogenetic depths at which temperature of
260 isolation was the dominant factor (pairwise nucleotide similarity range 0.957-0.986), suggesting
261 that seasonal *Methylobacterium* diversity dynamics could be partly driven by temperature
262 adaptation. We did not observe any significant effect of host tree species on *Methylobacterium*
263 isolate diversity, for any level of the phylogeny, suggesting no strong specific associations
264 between *Methylobacterium* strains and the tree species from which they were isolated.
265
266 We next asked specifically which nodes within the *Methylobacterium* phylogenetic tree were
267 associated with the two major factors contributing to overall diversity, namely forest and
268 temperature of isolation (**Figure 3a**). For every level in the *rpoB* phylogeny, we independently
269 tested for nodes (supported by at least 50% bootstrap) associated with forest of origin (SBL and
270 MSH) or temperature of isolation (20 and 30 °C) by permutation (100,000 permutations per level
271 and per factor; **Figure 3b**). We identified two nodes strongly associated with temperature of
272 isolation and corresponding to clades A6 (20 °C; $p<0.01$) and A9 (30 °C; $p<0.01$; **Figure 3b**).
273 Other clades were evenly isolated at 20 and 30 °C and we observed no significant association
274 between temperature of isolation and nodes embedded within clades. Nodes associated with
275 forest of origin also roughly corresponded to certain major clades, with clades A1+A2 and A10
276 almost exclusively sampled in MSH ($p<0.01$ and $p<0.05$, respectively). Clade A9 was isolated
277 significantly more often at SBL ($p<0.001$) but at least one of its subclades was significantly more
278 isolated at MSH ($p<0.05$), suggesting a relatively recent migration event. The fact that
279 *Methylobacterium* diversity typical of the phyllosphere show contrasted associations with forest
280 and temperature of isolation suggests that their evolution was tightly linked with processes
281 related to spatial and environmental variation including isolation by distance as well as niche-
282 based processes including adaptation to local climatic conditions.
283
284 *Comparison of Methylobacterium diversity assessed by rpoB barcoding and strain isolation*
285

286 To determine if these culture-based results were representative of the potentially uncultured
287 *Methylobacterium* diversity, we developed a culture-independent barcoded amplicon sequencing
288 approach based on *rpoB.* We performed *rpoB* amplicon sequencing for 184 leaf samples from 53
289 trees in both forests, allowed a monthly monitoring for most trees (**Table S3**). We identified 283
290 *Methylobacteriaceae rpoB* ASVs in these samples (**Figures S8-S11, Tables S10,S11**),
291 representing 24.6% of all sequences. Non-*Methylobacteriaceae* ASVs were mostly assigned to
292 other Rhizobiales families (850 ASVs, 70.33% of sequence abundance) and to Caulobacterales
293 (209 ASVs, 4.42% of sequence abundance) typical of the phyllosphere (see supplementary
294 information), suggesting that our *rpoB* marker is not limited to *Methylobacteriaceae* and can
295 potentially be used at a broader taxonomic scale. Within *Methylobacteriaceae*, ASVs were
296 mostly classified as *Methylobacterium* (200 ASVs, 23.05% of sequence relative abundance), and
297 *Enterovirga* (78 ASVs, 1.56%; **Table S12**). We assigned *Methylobacterium* ASVs to previously
298 defined clades using a maximum likelihood tree combining ASV sequences and reference
299 genomes (**Figure S12**). Most of *Methylobacterium* diversity was within the previously cultured
300 clades A9 (45.2% of *Methylobacterium* sequence abundance), A6 (24.3%), A1 (6.1%) and A10
301 (1.0%; **Table S13**). Estimates of *Methylobacterium* diversity based on *rpoB* sequences from
302 culture-independent sequencing or cultured isolates were generally concordant (**Table S13,**
303 **Figure S13**). Nevertheless, we cannot exclude the possibility that some diversity was not
304 isolated. For instance, although 19.1% of total *Methylobacterium* diversity assessed by *rpoB*
305 culture-free barcoding was assigned to group B, it only represented 4.8% of isolates. One
306 possible explanation could be adaptation of some isolates from this group to temperatures below
307 the range used for isolation (20-30 °C), as temperatures at the very beginning (May) and end
308 (October) of the growing period in Quebec typically range between 5 and 15°C.
309
310 *Fine-scale temporal and spatial distribution of Methylobacterium diversity assessed by rpoB*
311 *barcoding*
312
313 Our isolate-based survey suggested that the distribution of *Methylobacterium* diversity was
314 driven by both spatial and seasonal variation. This result was largely supported using the culture-
315 free approach (*rpoB* barcoding). Specifically, we found that spatial variation at both large
316 (distance between forests: 100km) and local scales (distance between plots within forest: 150-

317 1,200 m), as well as sampling date during the growing season (1-5 months), explained the largest
318 part of variance in the community composition of 200 *Methylobacterium* ASVs (proportion of
319 variation explained: 31.1%, 10.8% and 3.7%, respectively; p<0.001; PERMANOVA; Hellinger
320 transformation, Bray-Curtis dissimilarity, 10,000 permutations; **Table S14**). A majority of
321 *Methylobacterium* ASVs (124 out of 200) were significantly associated with one or either forest
322 (ANOVA; Bonferroni correction; **Figure 4a**), regardless their clade membership. The only
323 exception was observed for clade A1, which was almost exclusively observed (and isolated; see
324 **Figure 3b**) in the MSH forest. Also consistent without our isolation-based results, we found no
325 clear association between ASV or clade with host tree species, nor plots within forests (data not
326 shown).
327
328 To focus on temporal variation and fine-scale spatial effects, we removed large-scale spatial
329 variation by analyzing each forest separately. We quantified fine-scale spatial and temporal
330 dynamics of *Methylobacterium* diversity (200 ASVs), using autocorrelation analysis based on
331 Bray-Curtis dissimilarity index (*BC*). We observed a weak but significant decrease of community
332 similarity with geographical distance separating two samples within MSH (ANOVA on linear
333 model; $p<0.001$) but not SBL ($p>0.05$, **Table S15, Figure 4b**), and a significant decrease of
334 community similarity with time separating two samples in both forests (ANOVA on linear
335 model; $p<0.001$; **Table S15**), which was more marked in MSH than in SBL (**Figure 4c**). Both
336 results indicate that *Methylobacteriaceae* diversity is heterogeneously distributed even at very
337 local space and time scales. The overall community dissimilarity consistently decreased from
338 June to October in both MSH (from 0.624 to 0.297) and SBL (from 0.687 to 0.522; **Table S15,**
339 **Figure 4d**), suggesting that *Methylobacteriaceae* diversity was progressively homogenized by
340 migration or ecological filtering between the beginning and the end of the growing season at the
341 scale of a forest, although without affecting locally its heterogeneous spatial distribution in MSH
342 (**Table S15, Figure 4e**). The heterogeneous spatial distribution of *Methylobacterium* diversity
343 observed in MSH forest suggests either more restricted migration than in SBL, and/or local
344 adaptation due to environmental gradients. One possible explanation is that the floristic and
345 altitudinal gradient observed in MSH (**Figure 2d**) – but not in SBL – might generate local
346 adaptation to host tree species for *Methylobacterium* colonizing leaves in this more
347 heterogeneous forest, hence counteracting the homogenizing effect of neutral processes like

348 migration [49]. Accordingly, we found slight but significant effects of host tree species, and of the
349 interaction between host tree species and plots within forests, on *Methylobacterium* community
350 composition (each explaining 4.6% of variation in community composition; p<0.01%,
351 PERMANOVA; **Table S14**).
352
353 We tested for temporal autocorrelation in each node of the ML tree (**Figure S12**) supported by at
354 least 30% of bootstrapps (200 permutations) and observed significant temporal dynamics (as
355 attested by the positive slope between pairwise time and BC dissimilarity) in most testable nodes
356 (ANOVA, Bonferroni correction; **Figure 4f**). We observed the strongest temporal signals in
357 nodes embedded within clades A1 (MSH) and B (both forests), Accordingly, we found 25 ASVs
358 whose abundance significantly increased thourough the growing season (ANOVA; Bonferroni
359 correction; p<0.05), mostly belonging to clades A1 (n=11). Four ASVs increased significantly
360 with time in both forests and mostly belonged to group B (n=3), suggesting that at least a part of
361 the characteristics driving short-term dynamics of *Methylobacterium* communities are shared
362 among members of different clades within the genus.
363
364 *Effect of short scale temperature variation in combination with other environmental and genetic*
365 *factors on Methylobacterium growth performances*
366
367 A major environmental difference between forest sites and throughout the growing season relates
368 to shifts in temperature, suggesting, together with temperature preference of some clades during
369 the isolation step, that *Methylobacterium* diversity dynamics we observed over space and time
370 might result from clade contrasted growth performances under local climatic conditions. To
371 further explore the role of temperature, we measured growth of 79 *Methylobacterium* isolates
372 (sampled in 2018 in both forests; MSH: *n*=32, SBL: *n*=47 ; **Table S16**) for four temperature
373 treatments mimicking temperature variations during the growing season. Each treatment
374 consisted of an initial pre-conditioning step (*P*) during which each strain was incubated on solid
375 MMS media with methanol as sole carbon source for 20 days at either 20 °C (*P20*) or 30 °C
376 (*P30*), and a second monitoring step (*M*) during which pre-conditioned strains were incubated on
377 the same media and their growth monitored for 24 days at 20 °C (*P20M20* and *P20M30*) or 30 °C
378 (*P30M20* and *P30M30*; **Table S16, Figure S14**). Treatments *P20M20* and *P30M30* mimicked

379 stable thermal environments, and treatments *P20M30* and *P30M20* mimicked variable thermal
380 environments. For each isolate and temperature treatment, logistic growth curves were inferred
381 from bacteria spot intensity variation observed over three time points during the monitoring step
382 (**Figures S15, S16**). From growth curves, we estimated maximum growth intensity, or yield (*Y*)
383 and growth rate (*r*) as the inverse of lag+log time necessary to reach *Y* (**Figure S16, Table S16**
384 [50,51]). Clade membership explained a large part of variation in *Y* and *r* (30.6 and 7.6% of variation
385 explained, respectively; ANOVA; $p<0.001$), indicating that *Methylobacterium* growth
386 performance is largely long-term inherited and tends to be shared among clade members (**Figures**
387 **5a,b, Table 1**). Certain clades had a higher yield range than others, suggesting differences in their
388 carbon use efficiency [51], here provided by methanol. For example, group B isolates ($Y = 12.2 \pm$
389 5.0) have higher yield than group A ($Y = 5.4 \pm 3.5$). Different growth rates rather suggest
390 contrasted growth strategies across clades [51,52]. Strains from clades A1, A2 and B had the highest
391 growth rate (*r* range: 0.101±0.032 – 0.121±0.031), suggesting they have fast-growth strategy.
392 Other clades (A6, A9 and A10) had on average slower growth (*r* range: 0.082±0.021 –
393 0.088±0.024), suggesting that they have more efficient strategy [51].
394
395 Compared to clade membership, we observed that time of sampling, host tree species and forest
396 explained less variation in growth rate (5.4%, $p<0.001$; 2.2%, $p<0.01$ and 1.5%, $p<0.05$,
397 respectively; ANOVA; **Table 1**), suggesting that plasticity to the environment was a secondary
398 but still determining factor in strain growth strategy. The weak or non-significant interactions
399 between clade membership and the aforementioned environmental factors (ANOVA; **Table 1**)
400 suggest that these patterns were consistent across clades, indicating they are unlikely to result
401 from long-term adaptation but rather correspond to short-term responses to environmental
402 conditions. In both SBL and MSH, growth rate increased consistently from June (*r* =
403 0.075±0.018 and 0.085±0.033, respectively) to September/October (*r* = 0.097±0.031 and
404 0.103±0.027, respectively; **Figure 5c**). Growth rate increase thorough the season might result
405 from increasing competition within phyllosphere communities, for instance by selection for faster
406 growth. Accordingly, culture-independent *rpoB* confirmed that clades associated with faster
407 growth (clades B and A1) increased in abundance over time.
408

409 Temperature also had significant effects on growth performance. Temperature during the
410 monitoring phase explained respectively 2.0% and 15.8% of variation in yield and growth rate
411 (p<0.01 and p<0.001, respectively; ANOVA; **Figure 5d, Table 1**), regardless of clade
412 membership (no significant interaction in the ANOVA). Isolates incubated at 20 °C have on
413 average higher yield (Y=6.9±5.4) but slower growth (r=0.077±0.022) than isolates incubated at
414 30 °C (Y=4.9±3.6; r=0.100±0.030), suggesting that higher temperature tends to shift
415 *Methylobacterium* toward faster growth but lower efficiency, a typical trade-off observed in other
416 bacteria [51]. The effect of monitoring temperature on growth rate was also independent from time
417 of sampling (no significant interaction in the ANOVA), suggesting that *Methylobacterium* also
418 grow faster and less efficiently at 30 °C regardless temporal environmental variations.
419 Accordingly, the pre-conditioning temperature had no effect on growth rate (p>0.05; ANOVA),
420 and very limited on yield (1.4%; p<0.05; ANOVA), suggesting limited effect of short-time
421 temperature shift on *Methylobacterium* growth performance (**Table 1**).
422
423 **Discussion**
424
425 *Methylobacterium* is ubiquitous on leaves in the temperate forests of Québec and its diversity in
426 this habitat is quite similar to what has been described in the phyllosphere throughout the world,
427 with three main clades A9 (*M. brachiatum*, *M. pseudosasicola*), A6 (*M. sp.*) and A1 (*M.*
428 *gossipicola*) dominating diversity in the canopy. Our barcoding approach based on a clade-
429 specific *rpoB* marker revealed astonishing diversity within these clades, as well as within several
430 other clades: B (*M. extorquens*), A2 (*M. sp.*), A4 (*M. gnaphalii*, *M. brachytecii*) and A10 (*M.*
431 *komagatae*) whose importance in the phyllosphere has been underestimated by classical 16S
432 barcoding or strain isolation approaches. This diversity, like that of the overall phyllosphere
433 community, was mostly determined by differences between forests, with barcoding approaches
434 suggesting combined effects of restricted migration, local adaptation to host tree species, and
435 climatic conditions at large geographical scales (>100km). With higher molecular resolution, we
436 observed that *Methylobacterium* diversity was structured even at the scale of a forest (within 2
437 km), which according to a fine-scale timeline survey over the growing season also showed a clear
438 pattern of temporal dynamics and succesion. A finer analysis of *Methylobacterium* diversity
439 suggested that clade identity partly explained *Methylobacterium* geographical distribution at large

440 scale (forest) but not at finer scales (plots), nor was it an indicator of adaptation to a particular
441 host tree species, nor a determinant of temporal dynamics. Rather, the distribution of
442 *Methylobacterium* diversity at small temporal and geographical scales likely resulted from more
443 contemporaneous community assembly events selecting for phenotypic traits that evolved among
444 deeply diverging lineages of *Methylobacterium*, as has been observed in other bacterial [16] and
445 plant clades [53].
446
447 We explored mechanisms explaining the temporal dynamics of *Methylobacterium* diversity at the
448 scale of a growing season. Because we observed contrasting *Methylobacterium* isolable diversity
449 between 20 and 30 °C, we suspected that adaptation to temperature variation during the growing
450 season could explain part of these temporal dynamics. By monitoring *Methylobacterium* isolate
451 growth under different temperature treatments, we confirmed that temperature affected isolate
452 growth performances. The fact that most tested isolates grow slower but more efficiently at 20 °C
453 than at 30 °C (**Figure 5d**), regardless of their phylogenetic and environmental characteristics, is
454 in line with a temperature-dependent trade-off between growth rate and yield described in many
455 bacteria (reviewed in [51]). High yield strategies are typical of cooperative bacterial populations,
456 while fast growth-strategies are typical of competitive populations [51], suggesting that 20 °C is
457 likely closer to the thermal niche of a cooperative *Methylobacterium* community, in agreement
458 with average temperatures in temperate forests during the growing season. This observation also
459 stresses the importance of considering incubation temperature when interpreting results from
460 previous studies assessing *Methylobacterium* diversity based on strain isolation. We observed
461 several lines of evidence that factors other than direct adaptation to temperature drive
462 *Methylobacterium* responses to temperature variation, by affecting their growth strategy in
463 different competitive conditions rather than by affecting their metabolism directly. First, clade
464 identity was one of the main predictors of overall strain performance, with some clades (A1, A2,
465 B) possessing a rapid growth strategy under all temperature conditions, while others (clades A6,
466 A9, A10) had systematically slower growth. These clade-specific growth strategies could explain
467 for instance why certain *Methylobacterium* isolates are less competitive and less frequently
468 isolated at higher temperatures. Still, we cannot rule out that clade-specific growth strategy also
469 reflect experimental conditions. Second, we observed strong associations between strain growth
470 performance and time of sampling, regardless of clade association, suggesting that growth

471 dynamic strategies also respond to seasonal variations in environmental conditions, and to the
472 level of establishment and competition in the phyllosphere community [51]. This observation,
473 together with clade identity, could explain why, assuming that environmental conditions at the
474 end of the growing season became unfavorable for most strains, strains from clades A1 and B
475 with a fast-growth strategy consistently increase in frequency during this period and lead to the
476 homogeneization of the community. Taken together, our temporal survey of diversity dynamics
477 and screening for growth performance suggest the following timeline of the dynamics of the
478 *Methylobacterium* phyllosphere community. At the very beginning of the growing season, a pool
479 of bacteria with mixed ecological strategies and genotypes colonizes newly emerging leaves. Due
480 to the stochasticity of this colonization, we initially observe strong dissimilarity among
481 phyllosphere communities, regardless of their spatial position. During the summer, optimal
482 environmental conditions allow the progressive establishment of a cooperative and structured
483 bacterial community with a high yield strategy [51]. At the end of the growing season, with
484 migration, environmental conditions shifting and leaves senescing, strains with a fast-growth
485 strategy are able to grow rapidly, dominating the phyllosphere community and leading to its
486 homogeneization before leaves fully senesce.
487
488 Our study illustrates that *Methylobacterium* is a complex group of divergent lineages with
489 different ecological strategies and distributions, reflecting long-term adaptation to highly
490 contrasted environments. Based upon a similar observation, some authors recently proposed to
491 reclassify *Methylobacterium* group B within a new genus (*Methylorubrum*) that they argue is
492 ecologically and evolutionarily distinct from other *Methylobacterium* clades [30]. Although clade B
493 was well supported as a distinct clade in our analyses, our results suggest that it is in fact
494 embedded within clade A, which would render the genus *Methylobacterium* paraphyletic if clade
495 B is defined as a distinct genus, and group B was not particularly ecologically distinct in
496 comparison with other major clades. Our results emphasize the fact that torough genomic
497 investigations are needed to clarify the taxomonic status of *Methylobacterium*. Beyond any
498 taxonomic considerations, neither clade identity assessed by individual genetic markers nor the
499 tremendous ecological diversity among *Methylobacterium* clades can predict all of the spatial and
500 temporal variation in *Methylobacterium* diversity in nature. In order to define the niches of
501 *Methylobacterium* clades and to understand the metabolic mechanisms underlying their

502 contrasted life strategies, future characterization of their functions and genome structure will be
503 required using phylogenomic approaches.
504
505 In conclusion, we find that *Methylobacterium* adaptive responses to local environmental variation
506 in the phyllosphere are driven by both long-term inherited ecological strategies that differ among
507 major clades within the genus, as well by seasonal changes affecting habitat characteristics and
508 community structure in the phyllosphere habitat. Overall, our study combining sequencing- and
509 culture-based approaches provides novel insights into the factors driving fine-scale adaptation of
510 microbes to their habitats, and in the case of *Methylobacterium* our approach revealed the
511 particular importance of considering organismal life-history strategies to help understand the
512 small-scale diversity and dynamic of this ecologically important taxon.
513
514
515
516

517 **Figures and Table**

518

519 **Figure 1** - ***Methylobacterium* phylogeny and ecology.** Most of *Methylobacterium* diversity is found
520 in association with plants, especially in the phyllosphere. Maxium-Likelihood phylogenetic tree
521 (100 permutations, only nodes supported by at least 50% of bootstraps are shown) from *rpoB*
522 complete nucleotide sequences (4064 bp) available for 153 *Methylobacterium* genomes and
523 rooted on 32 *Methylobacteriaceae* outgroups (*Microvirga*, *Enterovirga*; no shown; see **Table**
524 **S1**). For each genome, the anthropogenic origin (black squares) and/or environmental origin are
525 indicated (color code on top left). Groups A, B, C adapted from [30]. Monophyletic clades within
526 group A (A1-A9) were defined using a ~92% nucleotide pairwise similarity cut-off on the *rpoB*
527 complete sequence (see **Figure S1**).

528

529 **Figure 2 - Sampling design.** a) Locations of the two sampled forests MSH (green) and SBL
530 (orange) in the province of Québec (Canada). b) Time line survey in each forest in 2018 (2-4 time
531 points available per tree). c-d). Detailed map of each forest and each plot within forests (squares;
532 6 to 10 trees were sampled per plot; see **Table S2,S3**). In MSH, plots H0 and L0 were sampled
533 once in 2017 for a pilot survey. In SBL and MSH, plots 1-6 were sampled 4 times in 2018. For
534 each plot, tree localizations are indicated by point colored according to their taxonomie (color
535 code on bottom left): ABBA (*Abies balsamea*), ACRU (*Acer rubrum*). ACSA (*Acer saccharum*),
536 OSVI (*Ostrya virginiana*), QURU (*Quercus rubra*), FAGR (*Fagus grandifolia*), ASPE (*Acer*
537 *Pennsylvanicum*). Shades of grey indicate elevation (50 m elevation scale)

538

539 **Figure 3 - Tests for phylogenetic association of traits with culture-based estimation of**
540 ***Methylobacterium* diversity.** a) Part of variance in *Methylobacterium* isolated diversity
541 explained by each trait and their interactions (PERMANOVA tests for association; 10,000
542 permutations; x-axis) in function of pairwise nucleotide similarity as a proxy for phylogenetic
543 depth (PS; y-axis). PERMANOVA were conducted at different depths within a maximum-
544 likelihood phylogenetic tree (100 bootstraps; nodes supported in less than 50% of replicated trees
545 were removed; legend on top right) drawn from partial *rpoB* nucleotide sequences of 187 isolates
546 (pilot survey in 2017: n=20; timeline survey in 2018: n=167) and 188 *Methylobacteriaceae*
547 reference sequences. The four following traits and their interactions were tested (see Venn

548 diagram on top left for color code): forest of origin, host tree species, sampling date and
549 temperature of isolation. Points indicate significant part of variance (legend on the left). b) Test
550 for node association (100,000 permutations) with forest of origin and temperature of isolation
551 (color code on top) mapped on the *rpoB* phylogeny (scaled on PS values; original tree in **Figure**
552 **S6**). Colored frames in the tree indicate nodes significantly associated with at least one factor
553 (ANOVA; Bonferonni correction; p<0.001: "***"; p<0.01:"**"; p<0.05:"*"). For each isolate
554 (names in bold), colored boxes at the tip of the tree indicate forest of origin and temperature of
555 isolation.
556
557 **Figure 4 - Short-scale spatial and temporal dynamics of *Methylobacterium* communities**
558 **assessed by *rpoB* barcoding.** a) A principal component analysis (PCA) on 200
559 *Methylobacterium* ASVs relative abundance (Hellinger transformation, Bray-Curtis (*BC*)
560 dissimilarity) shows that 184 phyllosphere samples (black points) cluster according to forest of
561 origin (MSH, SBL). The significant association of 124 ASVs with one or either forest (ANOVA,
562 Bonferonni correction; *p*<0.05; point size proportional to variance) is shown (points colored
563 according to clade assignation). b) Spatial and c) temporal autocorrelation analyzes conducted in
564 each forest separately. Points represent BC dissimilarity in function of pairwise geographic
565 (*pDist*; b) or pairwise time (*pTime*; c) distance separating two communities. For each forest and
566 variable, the predicted linear regression (*BC~pDIST* or *~pTime*) is indicated (full line: p<0.001;
567 dotted line: p>0.05; ANOVA). d) *BC* in function of sampling time for each forest. e) Detail of
568 spatial autocorrelation analyzes in MSH, conducted for each sampling time point separately. f)
569 Scaled ML tree (original tree from **Figure S12** scaled on pairwise nucleotide similarity (PS)) of
570 200 *Methylobacterium* ASV (points) and 176 reference *rpoB* sequences rooted on *Microvirga*
571 and *Enterovirga* (out group not shown). Temporal autocorrelation analyzes per forest were
572 conducted for each node supported by at least 30% of bootstraps (200 permutations). For each
573 forest and node, the strength of the slope (estimate of the linear regression *BC~pTime*;
574 proportional to point size) was displayed when highly significant (p<0.001; ANOVA, Bonferonni
575 correction).
576
577 **Figure 5 - Analysis of 79 *Methylobacterium* isolate growth performances under 4 different**
578 **temperature treatments.** For each strain and temperature treatment, the yield (*Y*: maximal

growth intensity) and growth rate (*r*; inverse of log+lag time) were estimated from growth curves. a) Average growth curves (growth intensity in function of time) for each clade (line: mean value; frame: 1/3 of standard deviation; point: average maximal growth). b) *r* in function of *Y*. Each point represents the average *r*/*Y* values for an isolate and a temperature treatment (79 isolates x 4 treatments), colored according to clade membership. Ellipsoides are centered on average values per clade and represent 30% of confidence interval (standard deviation). c) *r* (log scale) in function of time at which strains were isolated, colored according to the forest of origin. Points: real data; bars: average *r* value per forest (n=2) and time (n=4) category. d) *r* in function of Y, corrected for clade assignement (residuals of the *r*~Clade and *Y*~Clade linear regressions). Each point represents the average *r*/*Y* residual values for an isolate and a temperature treatment (79 isolates x 4 treatments), colored according to monitoring temperature (legend on top right).

592 **Table 1 - Part of variance in yield (*Y*) and growth rate (*r*) measured in 79 *Methylobacterium***
593 **strains grown under 4 temperature treatments.** *Y* and *r* values were transformed in log to meet
594 normal distribution. Significance of *Y* and *r* response were evaluated by ANOVA in linear
595 models: log(*Y*)~$F*H*D*T_p*T_M*C$ *and* log(*r*)~ $F*H*D*T_p*T_M*C$, respectively, with following
596 factors : clade (*C*), forest of origin (*F*), host tree species (*H*), time of sampling (*D*), temperature of
597 incubation during pre-conditioning (T_P) and monitoring (T_M) steps and their interactions (only
598 significant are shown: "***": p<0.00l; "**": p<0.01; "*": p<0.05).
599

	Rate	Yield
Forest (*F*)	0.015*	0.002
Host tree species (*H*)	0.022**	0.013**
Date of sampling (*D*)	0.054***	0.013**
Pre-conditioning temperature (*TP*)	0.001	0.014**
Monitoring temperature (*TM*)	0.158***	0.020**
Clade (*C*)	0.076***	0.306***
F:D	0.006	0.036***
H:D	0.001	0.015**
H:C	0.006	0.058***
D:C	0.032*	0.022*
F:H:D	0.019**	0.035***
F:H:C	0.013*	0.006
other interactions	0.142	0.084
Residuals	0.456	0.377

600
601

602 **List of supplementary information**

603

604 **Figure S1** - Validation of *Methylobacterium* group A subdivisions in nine clades.

605 **Table S1 -** List of reference *Methylobacteriaceae* genomes from which the complete *rpoB* and
606 *sucA* nucleotide sequences were available.

607 **Table S2 -** Description of sites of sampling.

608 **Table S3 -** Description of trees monitored in 2018 and sample usage.

609 **Figure S2 -** ASV rarefaction on diversity assessed by *16s* barcoding in 46 phyllosphere samples,
610 1 positive control (METH community) and 1 negative controls.

611 **Table S4** - Summary of 16S ASV taxonomic assignation using SILVA (v.138).

612 **Figure S3** - Main bacteria order distribution across 46 phyllosphere samples and one positive
613 control (METH community) in function of different factors.

614 **Figure S4** - Community analysis on bacterial diversity assessed from 16S barcoding in 46
615 phyllosphere samples.

616 **Table S5** - PERMANOVA analysis of variance in bacterial community diversity assessed from
617 16S barcoding in 46 phyllosphere samples

618 **Table S6 -** List of 76 strains isolated in MSH during a pilot survey in august 2017.

619 **Table S7** - Primers used to amplify hyper variable regions in genes *sucA* and *rpoB*.

620 **Figure S5 -** ML phylogenetic trees from *sucA* (a) and *rpoB* (b) concatenated hypervariable
621 regions.

622 **Table S8** - Information for 98 *Methylobacterium* strains successfully isolated, amplified and
623 sequenced for the *rpoB* marker from 2018 timeline (isolation batch 1/2).

624 **Table S9 -** Information for 69 *Methylobacterium* strains successfully isolated, amplified and
625 sequenced for the *rpoB* marker from 2018 timeline (isolation batch 2/2).

626 **Table S10 -** Information on 187 strains used for *rpoB* phylogeny, including 167 strains isolated
627 in 2018 and 20 strains isolated in 2017.

628 **Figure S6 -** ML tree on *rpoB* gene partial nucleotide sequences from 187 *Methylobacterium*
629 strain isolated in 2017 (n=20) and 2018 (n=167) and 188 *Methylobacteriaceae* reference
630 genomes.

631 **Figure S7 -** Iterative normalization of the *rpoB* phylogeny

632 **Figure S8** - Analysis of diversity in positive controls (METH communities) before ASVs
633 filtering and rarefaction.
634 **Figure S9 -** ASV rarefaction on diversity assessed by *rpoB* barcoding in 186 phyllosphere
635 samples, 4 positive controls (METH community) and 4 negative controls.
636 **Figure S10** - Diversity within METH communities after rarefaction.
637 **Table S11** - Summary of ASV taxonomic annotation before correction by *rpoB* phylogeny
638 **Figure S11** - Unrooted ML phylogenetic tree based on *rpoB* partial nucleotide sequences from
639 1,344 ASVs (410 bp).
640 **Table S12** - Summary of ASV taxonomic annotation after correction by *rpoB* phylogeny
641 **Figure S12** - Unrooted ML phylogenetic tree based on *rpoB* partial nucleotide sequences from
642 283 *Methylobacteriaceae* ASV (points) and 232 references strains and genomes (unlabeled tips).
643 **Table S13** - *Methylobacterium* ASV diversity and comparison with estimation from strain
644 isolation (2018).
645 **Figure S13** - Comparison of *Methylobacterium* diversity assessment from *rpoB* barcoding and
646 strain isolation.
647 **Table S14** - PERMANOVA analysis of 184 phyllosphere *Methylobacterium* samples assessed by
648 *rpoB* barcoding (200 ASVs).
649 **Table S15** - Summary of statistics from autocorrelation analyzes on 184 phyllosphere
650 *Methylobacterium* samples assessed by *rpoB* barcoding (200 ASVs).
651 **Table S16** - List of 79 *Methylobacterium* strains monitored for growth performance under four
652 temperature treatments
653 **Figure S14** - Experimental design of *Methylobacterium* monitoring for growth performance
654 under four temperature treatments.
655 **Figure S15** - Example of image analysis of *Methylobacterium* monitoring for growth
656 performance under four temperature treatments.
657 **Figure S16** - Prediction of log normal growth curve, growth rate and yield for 79 isolates
658 incubated under four temperature treatments.
659

660 **References**

661 1. Vorholt, J. A. Microbial life in the phyllosphere. *Nature Reviews Microbiology* **10**, 828–840
662 (2012).
663 2. Lindow, S. E. & Brandl, M. T. Microbiology of the Phyllosphere. *Appl. Environ. Microbiol.*
664 **69**, 1875–1883 (2003).
665 3. Fürnkranz, M. *et al.* Nitrogen fixation by phyllosphere bacteria associated with higher plants
666 and their colonizing epiphytes of a tropical lowland rainforest of Costa Rica. *The ISME*
667 *Journal* **2**, 561–570 (2008).
668 4. Laforest-Lapointe, I., Messier, C. & Kembel, S. W. Host species identity, site and time drive
669 temperate tree phyllosphere bacterial community structure. *Microbiome* **4**, 27 (2016).
670 5. Laforest-Lapointe, I., Messier, C. & Kembel, S. W. Tree phyllosphere bacterial communities:
671 exploring the magnitude of intra- and inter-individual variation among host species. *PeerJ* **4**,
672 e2367 (2016).
673 6. Noble, A. S., Noe, S., Clearwater, M. J. & Lee, C. K. A core phyllosphere microbiome exists
674 across distant populations of a tree species indigenous to New Zealand. *PLOS ONE* **15**,
675 e0237079 (2020).
676 7. Kembel, S. W. *et al.* Relationships between phyllosphere bacterial communities and plant
677 functional traits in a neotropical forest. *PNAS* **111**, 13715–13720 (2014).
678 8. Shade, A., Gregory Caporaso, J., Handelsman, J., Knight, R. & Fierer, N. A meta-analysis of
679 changes in bacterial and archaeal communities with time. *The ISME Journal* **7**, 1493–1506
680 (2013).
681 9. Malik, A. A. *et al.* Defining trait-based microbial strategies with consequences for soil carbon
682 cycling under climate change. *The ISME Journal* **14**, 1–9 (2020).
683 10. Moyes, A. B. *et al.* Evidence for foliar endophytic nitrogen fixation in a widely distributed

684 subalpine conifer. *New Phytologist* **210**, 657–668 (2016).

685 11. Lajoie, G. & Kembel, S. W. Making the Most of Trait-Based Approaches for Microbial
686 Ecology. *Trends in Microbiology* **27**, 814–823 (2019).

687 12. Nemergut, D. R. *et al.* Patterns and Processes of Microbial Community Assembly. *Microbiol.*
688 *Mol. Biol. Rev.* **77**, 342–356 (2013).

689 13. Cavender-Bares, J., Kozak, K. H., Fine, P. V. A. & Kembel, S. W. The merging of
690 community ecology and phylogenetic biology. *Ecology Letters* **12**, 693–715 (2009).

691 14. Martiny, J. B. H., Jones, S. E., Lennon, J. T. & Martiny, A. C. Microbiomes in light of traits:
692 A phylogenetic perspective. *Science* **350**, (2015).

693 15. Tromas, N. *et al.* The evolution of realized niches within freshwater Synechococcus.
694 *Environmental Microbiology* **22**, 1238–1250 (2020).

695 16. Tromas, N. *et al.* Niche Separation Increases With Genetic Distance Among Bloom-Forming
696 Cyanobacteria. *Front. Microbiol.* **9**, (2018).

697 17. Thompson, L. R. *et al.* A communal catalogue reveals Earth's multiscale microbial diversity.
698 *Nature* **551**, 457–463 (2017).

699 18. Poretsky, R., Rodriguez-R, L. M., Luo, C., Tsementzi, D. & Konstantinidis, K. T. Strengths
700 and Limitations of 16S rRNA Gene Amplicon Sequencing in Revealing Temporal Microbial
701 Community Dynamics. *PLOS ONE* **9**, e93827 (2014).

702 19. Ranjan, R., Rani, A., Metwally, A., McGee, H. S. & Perkins, D. L. Analysis of the
703 microbiome: Advantages of whole genome shotgun versus 16S amplicon sequencing.
704 *Biochemical and Biophysical Research Communications* **469**, 967–977 (2016).

705 20. Corpe, W. A. & Rheem, S. Ecology of the methylotrophic bacteria on living leaf surfaces.
706 *FEMS Microbiol Ecol* **5**, 243–249 (1989).

707 21. Keppler, F., Hamilton, J. T. G., Braß, M. & Röckmann, T. Methane emissions from terrestrial

708 plants under aerobic conditions. *Nature* **439**, 187–191 (2006).

709 22. Clarke, P. H. The biochemistry of Methylotrophs by C. Anthony Academic Press; London,
710 New York, 1982 xvi + 432 pages. £24.00, $49.50. *FEBS Letters* **160**, 303–303 (1983).

711 23. Anthony, C. Assimilation of carbon by methylotrophs. *Biotechnology* **18**, 79–109 (1991).

712 24. Ivanova, E. G., Doronina, N. V. & Trotsenko, Yu. A. Aerobic Methylobacteria Are Capable
713 of Synthesizing Auxins. *Microbiology* **70**, 392–397 (2001).

714 25. Madhaiyan, M. *et al.* Pink-pigmented facultative methylotrophic bacteria accelerate
715 germination, growth and yield of sugarcane clone Co86032 (Saccharum officinarum L.). *Biol*
716 *Fertil Soils* **41**, 350–358 (2005).

717 26. Madhaiyan, M., Poonguzhali, S. & Sa, T. Metal tolerating methylotrophic bacteria reduces
718 nickel and cadmium toxicity and promotes plant growth of tomato (Lycopersicon esculentum
719 L.). *Chemosphere* **69**, 220–228 (2007).

720 27. Dourado, M. N., Aparecida Camargo Neves, A., Santos, D. S. & Araújo, W. L.
721 Biotechnological and Agronomic Potential of Endophytic Pink-Pigmented Methylotrophic
722 Methylobacterium spp. *Biomed Res Int* **2015**, (2015).

723 28. Ryu, J. H. (Chungbuk N. U. *et al.* Plant Growth Substances Produced by Methylobacterium
724 spp. and Their Effect on Tomato (Lycopersicon esculentum L.) and Red Pepper (Capsicum
725 annuum L.) Growth. *Journal of Microbiology and Biotechnology* (2006).

726 29. Lee, H. S. *et al.* Physiological enhancement of early growth of rice seedlings (Oryza sativa
727 L.) by production of phytohormone of N2-fixing methylotrophic isolates. *Biol Fertil Soils* **42**,
728 402–408 (2006).

729 30. Green, P. N. & Ardley, J. K. Review of the genus Methylobacterium and closely related
730 organisms: a proposal that some Methylobacterium species be reclassified into a new genus,
731 Methylorubrum gen. nov. *International Journal of Systematic and Evolutionary*

732 *Microbiology* **68**, 2727–2748 (2018).

733 31. Chen, W.-M., Cai, C.-Y., Li, Z.-H., Young, C.-C. & Sheu, S.-Y. Methylobacterium
734 oryzihabitans sp. nov., isolated from water sampled from a rice paddy field. *International*
735 *Journal of Systematic and Evolutionary Microbiology,* **69**, 3843–3850 (2019).

736 32. Feng, G.-D. *et al.* Methylobacterium nonmethylotrophicum sp. nov., isolated from tungsten
737 mine tailing. *International Journal of Systematic and Evolutionary Microbiology,* **70**, 2867–
738 2872 (2020).

739 33. Jia, L. juan *et al.* Methylobacterium crusticola sp. nov., isolated from biological soil crusts.
740 *International Journal of Systematic and Evolutionary Microbiology,* **70**, 2089–2095 (2020).

741 34. Kim, J. *et al.* Methylobacterium terricola sp. nov., a gamma radiation-resistant bacterium
742 isolated from gamma ray-irradiated soil. *International Journal of Systematic and*
743 *Evolutionary Microbiology,* **70**, 2449–2456 (2020).

744 35. Kim, J., Chhetri, G., Kim, I., Kim, M. K. & Seo, T. Methylobacterium durans sp. nov., a
745 radiation-resistant bacterium isolated from gamma ray-irradiated soil. *Antonie van*
746 *Leeuwenhoek* **113**, 211–220 (2020).

747 36. Ten, L. N. *et al.* Methylobacterium segetis sp. nov., a novel member of the family
748 Methylobacteriaceae isolated from soil on Jeju Island. *Arch Microbiol* **202**, 747–754 (2020).

749 37. Jiang, L. *et al.* Methylobacterium planium sp. nov., isolated from a lichen sample. *Arch*
750 *Microbiol* **202**, 1709–1715 (2020).

751 38. Pascual, J. A. *et al.* Methylobacterium symbioticum sp. nov., a new species isolated from
752 spores of Glomus iranicum var. tenuihypharum. *Curr Microbiol* **77**, 2031–2041 (2020).

753 39. Marx, C. J. *et al.* Complete Genome Sequences of Six Strains of the Genus
754 Methylobacterium. *J Bacteriol* **194**, 4746–4748 (2012).

755 40. Tani, A., Ogura, Y., Hayashi, T. & Kimbara, K. Complete Genome Sequence of

756 Methylobacterium aquaticum Strain 22A, Isolated from Racomitrium japonicum Moss.
757 *Genome Announc.* **3**, (2015).
758 41. Minami, T. *et al.* Complete Genome Sequence of Methylobacterium sp. Strain AMS5, an
759 Isolate from a Soybean Stem. *Genome Announc.* **4**, (2016).
760 42. Morohoshi, T. & Ikeda, T. Complete Genome Sequence of Methylobacterium populi P-1M,
761 Isolated from Pink-Pigmented Household Biofilm. *Genome Announc.* **4**, (2016).
762 43. Belkhelfa, S. *et al.* Complete Genome Sequence of the Facultative Methylotroph
763 Methylobacterium extorquens TK 0001 Isolated from Soil in Poland. *Genome Announc.* **6**,
764 (2018).
765 44. Vos, M., Quince, C., Pijl, A. S., Hollander, M. de & Kowalchuk, G. A. A Comparison of
766 rpoB and 16S rRNA as Markers in Pyrosequencing Studies of Bacterial Diversity. *PLOS*
767 *ONE* **7**, e30600 (2012).
768 45. Ogier, J.-C., Pagès, S., Galan, M., Barret, M. & Gaudriault, S. rpoB, a promising marker for
769 analyzing the diversity of bacterial communities by amplicon sequencing. *BMC Microbiol*
770 **19**, 171 (2019).
771 46. Callahan, B. J. *et al.* DADA2: High resolution sample inference from Illumina amplicon data.
772 *Nat Methods* **13**, 581–583 (2016).
773 47. Green, P. N. Methylobacterium. in *Bergey's Manual of Systematics of Archaea and Bacteria*
774 1–8 (American Cancer Society, 2015). doi:10.1002/9781118960608.gbm00830.
775 48. Charron, G., Leducq, J. B., Bertin, C., Dube, A. K. & Landry, C. R. Exploring the northern
776 limit of the distribution of Saccharomyces cerevisiae and Saccharomyces paradoxus in North
777 America. *FEMS Yeast Res* **14**, 281–8 (2014).
778 49. Leducq, J. B. *et al.* Local climatic adaptation in a widespread microorganism. *Proceedings.*
779 *Biological sciences / The Royal Society* **281**, 20132472 (2014).

50. Zwietering, M. H., Jongenburger, I., Rombouts, F. M. & Riet, K. van ’t. Modeling of the Bacterial Growth Curve. *Appl. Environ. Microbiol.* **56**, 1875–1881 (1990).

51. Lipson, D. A. The complex relationship between microbial growth rate and yield and its implications for ecosystem processes. *Front Microbiol* **6**, (2015).

52. MacArthur, R. H. & Wilson, E. O. *The Theory of Island Biogeography*. (Princeton University Press, 2001).

53. Cavender-Bares, J., Ackerly, D. D., Baum, D. A. & Bazzaz, F. A. Phylogenetic Overdispersion in Floridian Oak Communities. *The American Naturalist* **163**, 823–843 (2004).

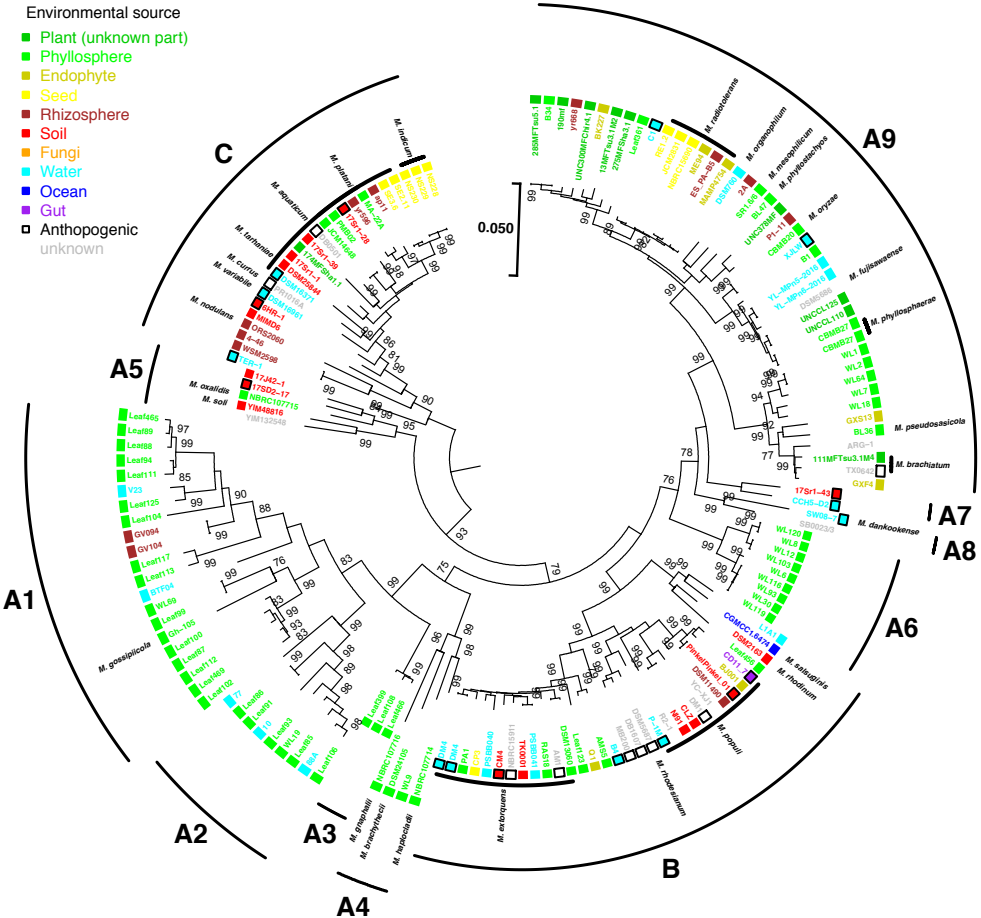

Environmental source
Plant (unknown part)
Phyllosphere
Endophyte
Seed
Rhizosphere
Soil
Fungi
Water
Ocean
Gut
Anthopogenic
unknown
0.050
A1
A2
A3
A4
A5
A6
A7
A8
A9
B
C
M. indicum
M. platani
M. sequaticum
M. tarhanlae
M. currus
M. variabile
M. nodulans
M. oxalidis
M. soli
M. gossipicola
M. gnaphalii
M. brachytheci
M. hapiocladii
M. exterquens
M. rhodesianum
M. populi
M. salauginis
M. rhodinum
M. dankookense
M. brachiatum
M. pseudosasicola
M. phyllosphaerae
M. fujisawaense
M. oryzae
M. mesophilicum
M. phyllostachyos
M. organophilum
M. radiotolerans

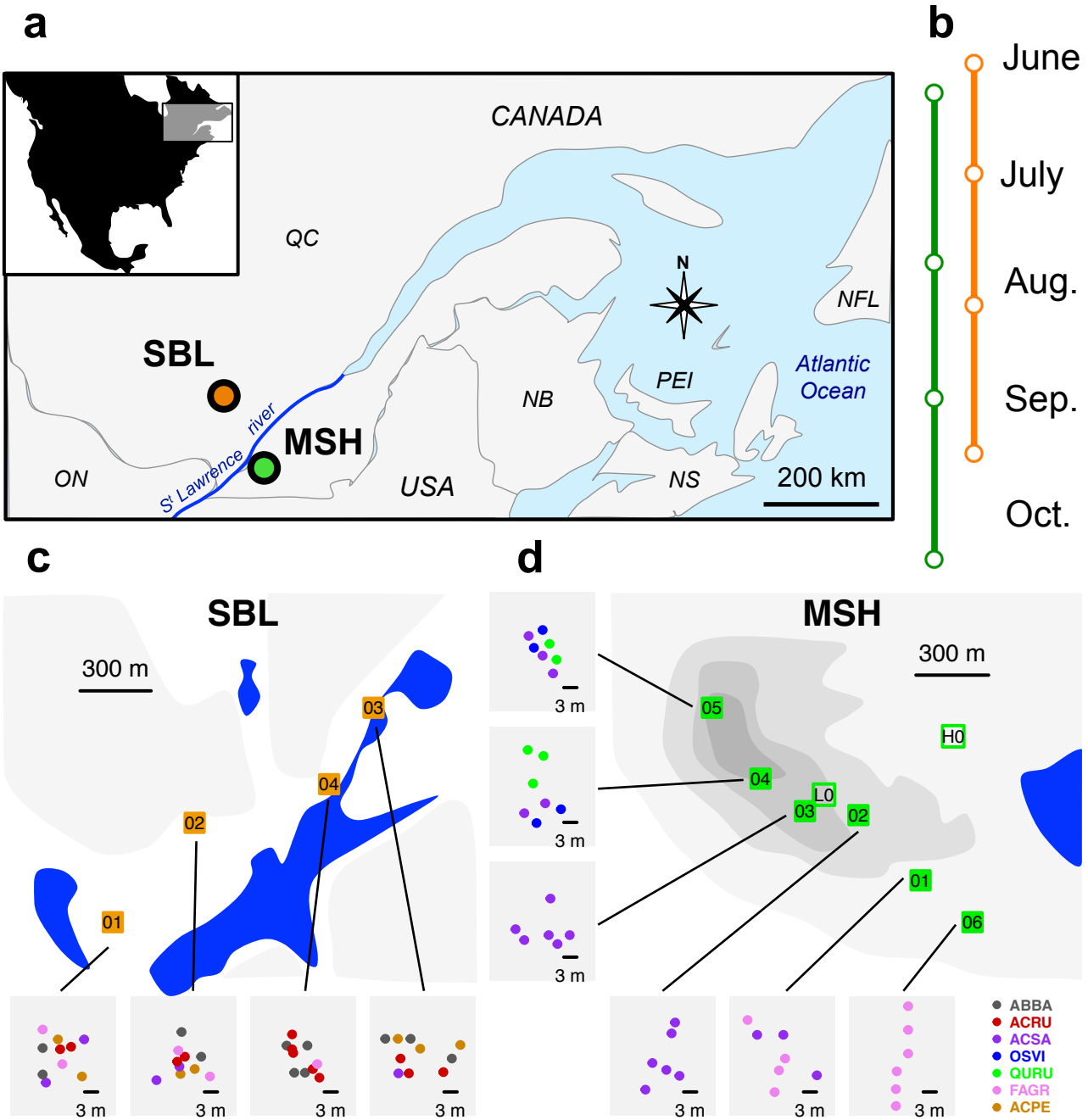
a
CANADA
QC
SBL
MSH
S' Lawrence river
ON
USA
NB
PEI
NS
NFL
Atlantic Ocean
N
200 km
b
June
July
Aug.
Sep.
Oct.
c
SBL
300 m
01
02
03
04
3 m
d
MSH
300 m
05
04
03
02
01
06
H0
L0
3 m
ABBA
ACRU
ACSA
OSVI
QURU
FAGR
ACPE

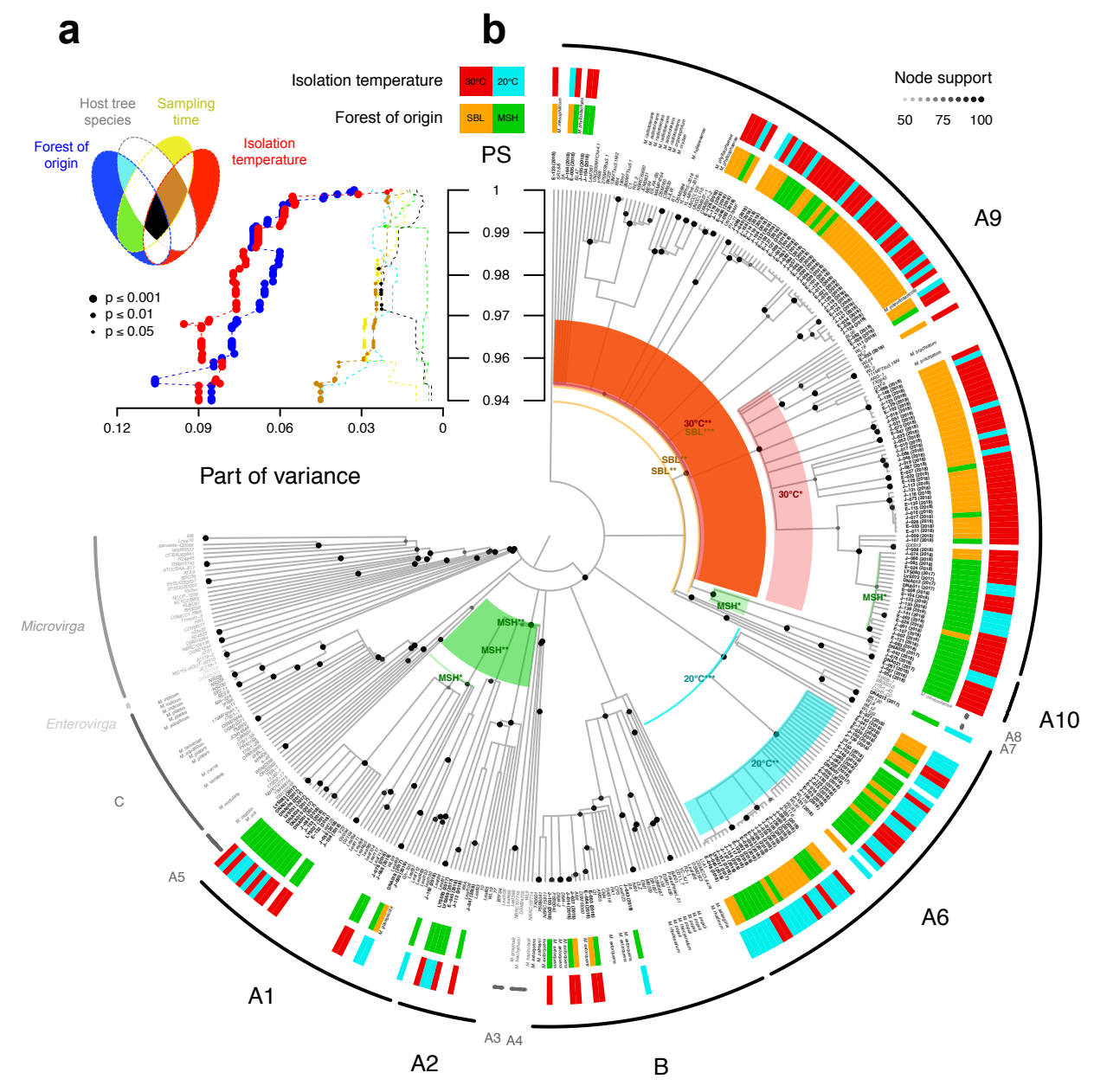
a
b
Host tree species
Sampling time
Forest of origin
Isolation temperature
Part of variance
p ≤ 0.001
p ≤ 0.01
p ≤ 0.05
0.12
0.09
0.06
0.03
0
PS
1
0.99
0.98
0.97
0.96
0.94
Isolation temperature
30°C
20°C
Forest of origin
SBL
MSH
Node support
50
75
100
A9
A10
A8
A7
A6
A5
A1
A2
A3
A4
B
C
Microvirga
Enterovirga
30°C**
SBL***
SBL**
SBL*
30°C*
MSH*
MSH*
MSH*2
MSH**
MSH*
20°C***
20°C**

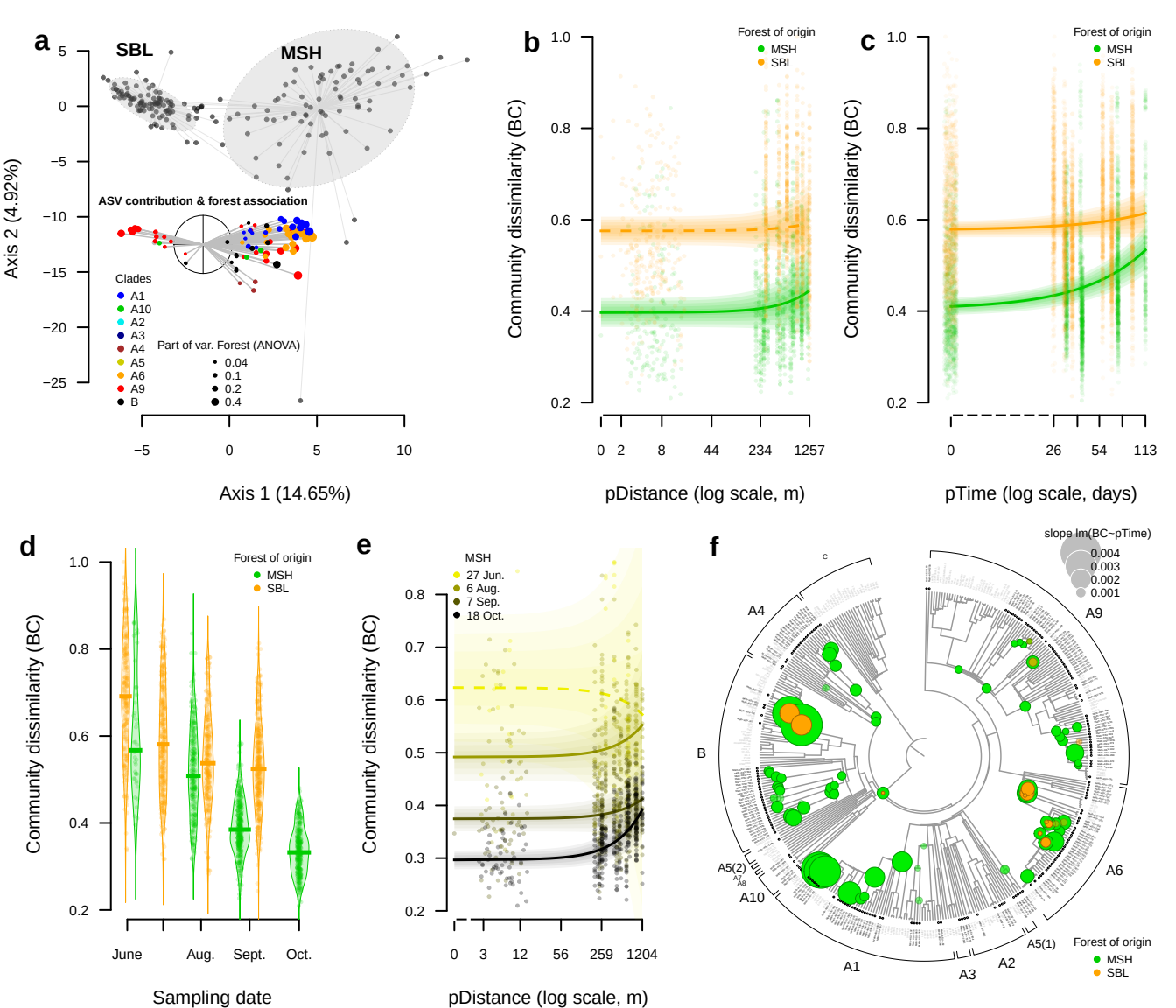
a
SBL
MSH
ASV contribution & forest association
Clades
A1
A10
A2
A3
A4
A5
A6
A9
B
Part of var. Forest (ANOVA)
0.04
0.1
0.2
0.4
Axis 2 (4.92%)
Axis 1 (14.65%)
b
Forest of origin
MSH
SBL
Community dissimilarity (BC)
pDistance (log scale, m)
c
Forest of origin
MSH
SBL
Community dissimilarity (BC)
pTime (log scale, days)
d
Forest of origin
MSH
SBL
Community dissimilarity (BC)
June
Aug.
Sept.
Oct.
Sampling date
e
MSH
27 Jun.
6 Aug.
7 Sep.
18 Oct.
Community dissimilarity (BC)
pDistance (log scale, m)
f
slope lm(BC~pTime)
0.004
0.003
0.002
0.001
A4
A9
B
A5(2)
A10
A6
A5(1)
A1
A3
A2
Forest of origin
MSH
SBL

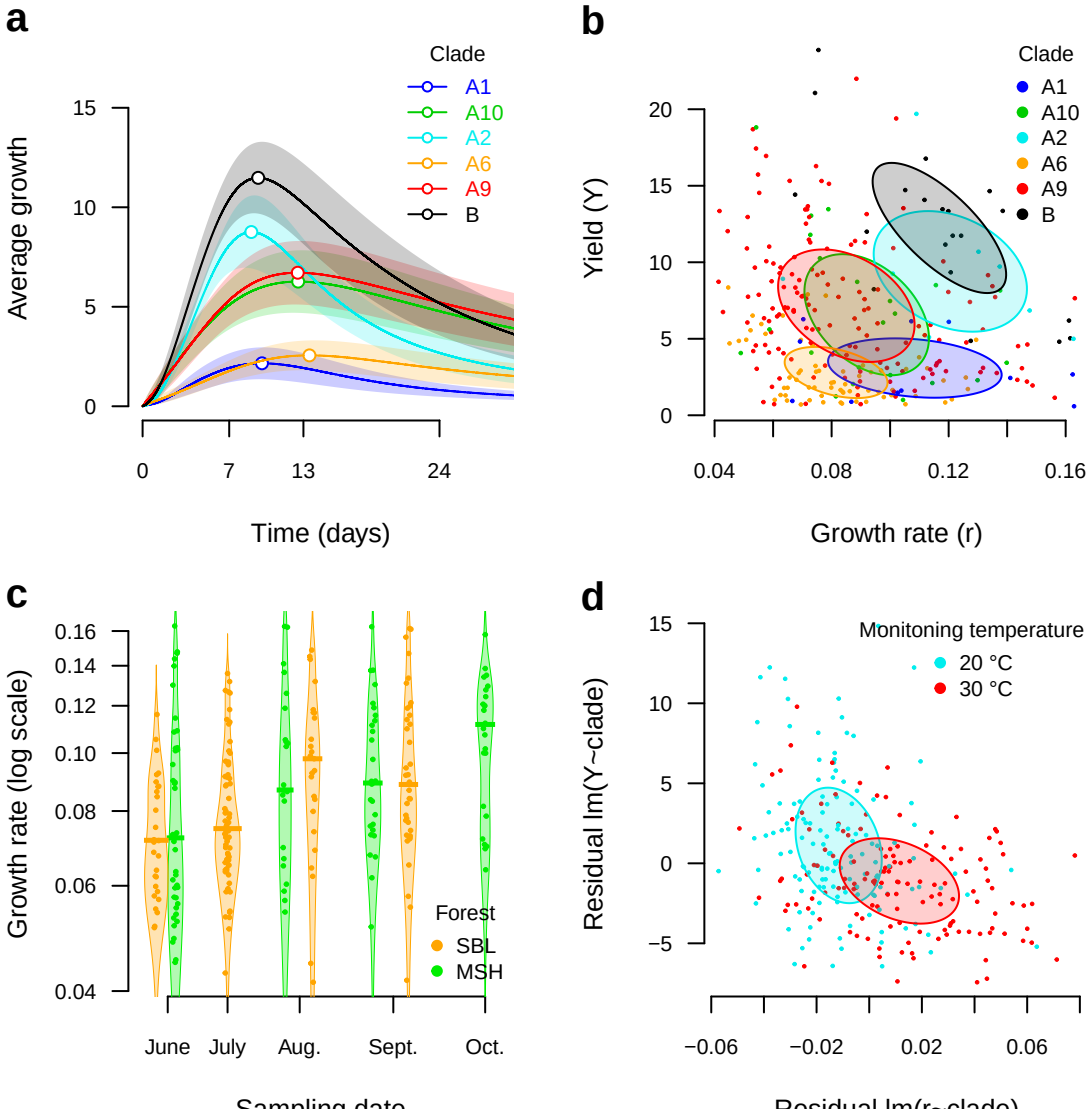
a
Clade
A1
A10
A2
A6
A9
B
Average growth
15
10
5
0
0
7
13
24
Time (days)
b
Clade
A1
A10
A2
A6
A9
B
Yield (Y)
20
15
10
5
0
0.04
0.08
0.12
0.16
Growth rate (r)
c
Growth rate (log scale)
0.16
0.14
0.12
0.10
0.08
0.06
0.04
Forest
SBL
MSH
June
July
Aug.
Sept.
Oct.
Sampling date
d
Monitoning temperature
20 °C
30 °C
Residual lm(Y~clade)
15
10
5
0
−5
−0.06
−0.02
0.02
0.06
Residual lm(r~clade)